Synthetic Challenges in the Assembly of Macrocyclic HCV NS3/NS4A Protease Inhibitors: The Case of BILN 2061 and Its Analogs

Youla S. Tsantrizos

Abstract The virally encoded serine protease NS3/NS4A is essential for the life cycle of the hepatitis C virus (HCV), an important human pathogen causing chronic hepatitis, cirrhosis of the liver, and hepatocellular carcinoma. The quest for the discovery of antiviral agents targeting the NS3/NS4A was initiated with a substrate-based hexapeptide as the lead structure. Evaluation of the conformational pre-organization of this ligand to the bioactive conformation led to the design of macrocyclic peptides, typified by the antiviral agents BILN 2061. Today, closely related analogs of BILN 2061 represent an important class of human therapeutics for the treatment of HCV infection. The critical steps in the synthesis of these compounds involves the cyclization of a tripeptide diene, containing a (1R,2S)-vinyl aminocyclopropylcarboxylate residue, via ring-closing metathesis (RCM). Conformational factors, ligand effects, and reaction conditions were evaluated, and a protocol was developed for the efficient production of these peptidomimetics in high yield and diastereomeric purity. The assembly of these challenging molecules and the key optimization studies are described.

Keywords Hepatitis C virus · Macrocyclic peptides · NS3/NS4A protease inhibitors

Contents

Y.S. Tsantrizos (✉)
Department of Chemistry, McGill University, 801 Sherbrooke Street West, Montreal, QC, Canada, H3A 0B8
e-mail: youla.tsantrizos@mcgill.ca

Abbreviations

Ac	Acetyl
ACCA	1-Aminocyclopropanecarboxylic acid
API	Active pharmaceutical ingredient
aq	Aqueous
BI	Boehringer Ingelheim
Bn	Benzyl
Boc	*tert*-Butoxycarbonyl
cod	Cyclooctadiene
Cy	Cyclohexyl
DEAD	Diethyl azodicarboxylate
DIAD	Diisopropyl azodicarboxylate
DIPEA	*N,N*-Diisopropylethylamine
DMF	Dimethylformamide
(*S,S*)-Et-DUPHOS	1,2-Bis[(2*S*,5*S*)-2,5-diethylphospholano]benzene
EC_{50}	Half maximal effective concentration
equiv	Equivalent(s)
Et	Ethyl
FDA	Food and Drug Administration
h	Hour(s)
HCV	Hepatitis C virus
HPLC	High-performance liquid chromatography
HTS	High-throughput screening
i-Bu	Isobutyl
IC_{50}	Half maximal inhibitory concentration
IFN-α	Pegylated interferon alpha
KHMDS	Potassium hexamethyldisilazide, potassium bis(trimethylsilyl) amide
LC–MS	Liquid chromatography–mass spectrometry
LiHMDS	Lithium hexamethyldisilazide, lithium bis(trimethylsilyl)amide
Me	Methyl
mol	Mole(s)
MTBE	Methyl *tert*-butyl ether
n-Bu	Butyl

NMR	Nuclear magnetic resonance
NS3	Nonstructural protein 3
Ph	Phenyl
PNBA	*p*-Nitrobenzoic
ppm	Parts per million
RCM	Ring-closing metathesis
RNA	Ribonucleic acid
ROESY	Rotating-frame Overhauser effect spectroscopy
rt	Room temperature
SAR	Structure–activity relationships
S_N2	Substitution nucleophilic (bimolecular)
TBTU	*N,N,N′,N′*-Tetramethyl-*O*-(benzotriazol-1-yl)uronium tetrafluoroborate
t-Bu	*tert*-Butyl
Tf	Trifluoromethanesulfonyl (triflyl)
THF	Tetrahydrofuran
TON	Turnover number
Vinyl ACCA	1-Amino-2-vinylcyclopropanecarboxylic acid

1 Introduction

In 1989, Chiron sequenced the genome of the hepatitis C virus (HCV) and identified HCV as the agent causing non-A, non-B hepatitis in humans [1]. Although HCV infections can remain asymptomatic for many years (~20 years), the majority of infected individuals (>80%) become chronically infected and usually progress to end-stage liver diseases that may eventually lead to hepatocellular carcinomas (~2–4%). Due to the significant HCV-related health burden worldwide (an estimated 170 million people chronically infected), numerous pharmaceutical industries invested heavily in the discovery of antiviral agent for treating this infection. Initially, progress was very slow, as understanding of the HCV biology proved to be an extremely challenging endeavor [2].

The first options for treating HCV were limited to pegylated interferons (IFN-α) [3] in combination with the broad-spectrum/nonselective antiviral nucleoside ribavirin [4]. However, this treatment was associated with severe side effects, and sustained reduction in viral load was achieved in only half of patients infected with HCV genotype 1a/b, the most prevalent genotype (~70%) in industrialized nations. Therefore, there was an urgent need for more effective and specific anti-HCV drugs targeting specific virally encoded enzymes that are essential for viral replication.

The HCV genome (a positive single-stranded RNA of ~9,600 nucleotides) encodes a precursor polypeptide of approximately 3,000 amino acids. This polyprotein is processed both co- and posttranslationally to produce structural (C, E1, E2, p7) and nonstructural (NS2, NS3, NS4A, NS4B, NS5A, NS5B) proteins [2]. Key nonstructural proteins include the NS3 protease enzyme (the N-terminal

Table 1 Compounds currently approved for the treatment of HCV infections

Compound	Approved	Lead companies	Target
Telaprevir[a]	2011	Vertex/J&J	NS3/NS4A
Boceprevir[a]	2011	Schering-Plough/Merck	
Simeprevir	2013	Medivir/J&J	
Paritaprevir	2014	Abbott(AbbVie)/Enanta	
Sofosbuvir	2013	Gilead	NS5B
Dasabuvir	2014	Abbott	
Daclatasvir	2014	Bristol-Myers Squibb	NS5A
Ledipasvir	2014	Gilead	
Ombitasvir	2014	AbbVie	

[a]These activated carbonyl derivatives act as reversible covalent inhibitors of the NS3/NS4A; they exhibit significantly lower potency and oral bioavailability compared to the macrocyclic inhibitors simeprevir and paritaprevir, and their use has been discontinued [7]

domain of the NS3 protein) and the RNA-dependent RNA polymerase enzyme (NS5B); in vitro and ex vivo studies have validated both as therapeutic targets. For example, abrogating the catalytic function of the NS3 protease results in HCV clones that have lost their infectivity. Between 1995 and 2014, an estimated 712 unique drug discovery programs were initiated worldwide. To date, only nine selective inhibitors targeting a virally encoded HCV protein have been approved in the major markets (Table 1) [5]. Most of these compounds target the NS3/NS4A serine protease (4A is a short peptide that serves as a cofactor of the NS3 protease) and the NS5B RNA-dependent RNA polymerase. Interestingly, although the NS5A protein lacks enzymatic activity and its role in viral replication remains unclear, compounds that bind to this protein can also efficiently block HCV replication [6].

This chapter focuses on the design and synthesis of the macrocyclic inhibitors of the HCV NS3/NS4A serine protease, typified by the first clinically validated analog BILN 2061 (**7**). This class of compounds provided clinical validation for HCV-specific small-molecule antiviral agent targeting the NS3/NS4A protease. Numerous structurally related analogs have been under investigation by pharmaceutical industries worldwide. Recently, simeprevir (**13**) and paritaprevir (**14**) received FDA approval for the treatment of HCV infections (Table 1).

2 Structure-Based Design of Peptidomimetic Inhibitors of the NS3/NS4A Serine Protease

The HCV NS3 serine protease is responsible for the proteolytic processing of four out of five junctions along the nonstructural region of the HCV polyprotein and plays an essential role in viral replication. It is a heterodimeric enzyme that requires a non-covalent association with the NS4A cofactor peptide for its optimal catalytic function. Furthermore, this enzyme silences the host's antiviral immune response,

blocking the host's natural defense against infections [8]. Therefore, it is not surprising that the NS3/NS4A has been a primary target for drug discovery for over 20 years.

In spite of major investments by many pharmaceutical industries [9], high-throughput screening (HTS) failed to identify small molecules capable of inhibiting the NS3/NS4A protease; this is likely due to the enzyme's very shallow and solvent-exposed active site cavity. Contrary to conventional wisdom advocating against peptidomimetics (on the basis of their well-known poor oral bioavailability and rapid excretion), in the early 1990s, Boehringer Ingelheim (BI) [10] and the Istituto di Ricerche di Biologia Molecolare [11] independently began to explore hexapeptide inhibitors of the NS3/NS4A. Compounds such as peptide **1**, mimicking the N-terminal cleavage products derived from the HCV polyprotein substrate, became the lead structures for medicinal chemists (Fig. 1) [reference from P1 (cleavage site) to P6 for the amino acid residues is based on the terminology used to indicate protease specificity] [12]. Additionally, hexapeptides **1** and **2** were used as molecular tools to explore the interactions between these ligands and the NS3 protease domain by NMR and molecular modeling [13–15]. Although the inherent conformational flexibility of linear hexapeptides magnified the challenges of drug discovery, potent tetrapeptide inhibitors of the NS3/NS4A (**3** and **4**) were eventually identified [16, 17]. However, in spite of their significant intrinsic potency (e.g.,
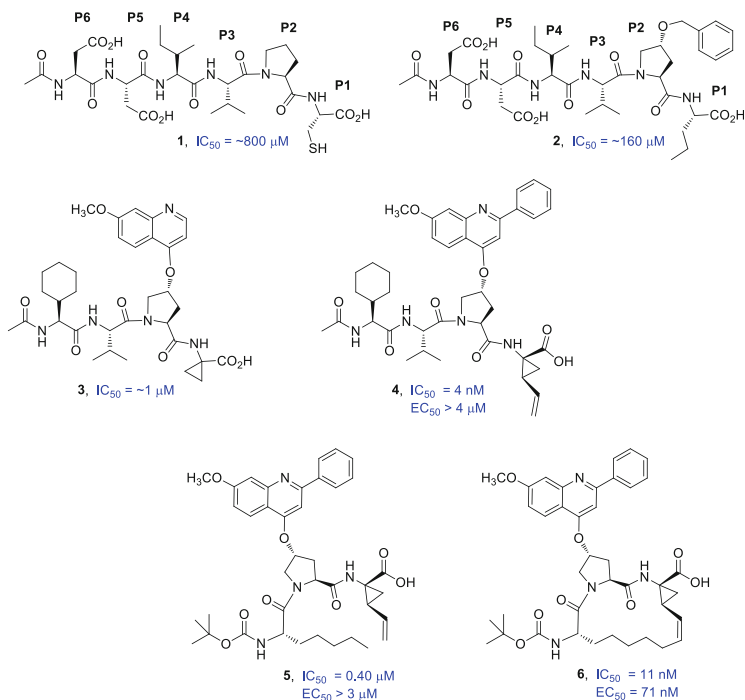

Fig. 1 Progression of the early structure–activity relationship studies

compound **4** has an IC$_{50}$ of 4 nM), these acyclic analogs did not exhibit any appreciable antiviral potency in the human hepatoma (Huh-7) sub-genomic HCV RNA replicon assay (the only validated tool for assessing antiviral efficacy at that time) [18].

In-depth investigation of the essential structural elements for favorable ligand–protein interactions led to the design of highly potent macrocyclic inhibitors of the NS3/NS4A [19]. For example, design of analog **6** (Fig. 1) was guided by the NMR data of the enzyme-bound hexapeptide **2**, indicating that the P3 side chain of **2** binds on the solvent-exposed surface of the protein and in close proximity to the P1 side chain, whereas the P5 and P6 residues did not interact with the protein [13]. The 15-membered ring tripeptide scaffold was designed to adopt in the *free state* the enzyme-bound secondary structure of hexapeptide **2**, forcing the P2–P3 amide bond to adopt exclusively the *trans* geometry preferred for binding [19]; this is in contrast to the linear proline-containing peptides that exist as mixtures of *cis*- and *trans*-rotamers. Furthermore, it was anticipated that the reduction in the conformational entropic penalty paid upon binding of the macrocyclic peptide to the enzyme could contribute in an overall favorable binding energy. Lastly, inspired by nature's macrocyclic peptides (e.g., cyclosporine, vancomycin), the 15-membered ring inhibitors of HCV NS3/NS4A protease were expected to exhibit better biopharmaceutical properties than their corresponding linear analogs. Gratifyingly, we found that analog **6**, having the P1 vinyl moiety tethered to the P3 side chain via a hydrocarbon linker, exhibited low nanomolar potency in inhibiting the enzyme (IC$_{50}$ = 11 nM), as well as blocking replication of HCV sub-genomic RNA in the cell-based replicon assay (EC$_{50}$ = 71 nM) [19]. In contrast, its corresponding acyclic analog **5** was almost 40-fold less potent in the enzymatic assay and completely inactive in the cell-based replicon assay at the highest concentration that it could be tested (Fig. 1) [19, 20].

Further optimization of the prototype molecule **6** led to the first clinical candidate, BILN 2061 (**7**), targeting the HCV NS3/NS4A protease (Fig. 2) [21, 22]. Following the disclosure of these compounds by BI and the favorable Phase I clinical data of **7**, demonstrating its exceptional efficacy in reducing the viral load of HCV-infected patients, the macrocyclic scaffold was enthusiastically adopted in this field of HCV drug discovery (e.g., more than 60 patents on macrocyclic HCV NS3/NS4A inhibitors have been filed by many pharmaceutical companies). In the following years, numerous structurally related preclinical and clinical candidates were reported by pharmaceutical companies worldwide, including analogs **8–14** (Fig. 2). Two compounds, simeprevir (**13**) and paritaprevir (**14**), were recently approved as therapeutic agent in the treatment of hepatitis C infections in humans (Fig. 2).
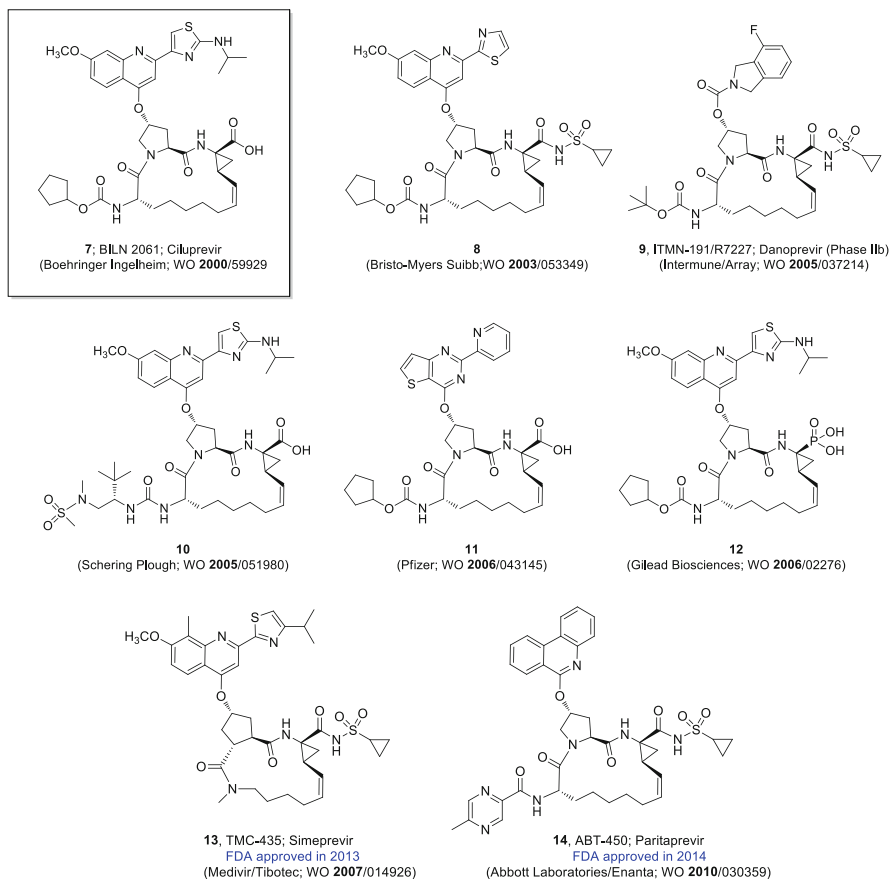
Fig. 2 Macrocyclic inhibitors of the HCV NS3/NS4A protease; examples of exploratory, pre-clinical, clinically validated, and approved drugs

3 Efficient Large-Scale Synthesis of Macrocyclic Inhibitors of HCV NS3/NS4A Protease

Initially, the production of multi-kilogram quantities of a complex macrocyclic compound, such as BILN 2061 (**7**), presented enormous synthetic challenges, and failure to address these challenges would certainly prevent commercialization of this important class of human therapeutics. Retrosynthetic analysis of BILN 2061 (**7**) suggested that the macrocyclic backbone could be formed via ring-closing metathesis of an acyclic tripeptide diene (Fig. 3). Developing cost-efficient protocols for the preparation of each key building block (i.e., P1, P2, and P3), as well as assembling the macrocyclic tripeptide, was critical. After numerous modifications/optimizations of the synthetic methodologies implicated in Fig. 3, BILN 2061 (**7**) was synthesized in high efficiency and in multi-kilogram quantities.
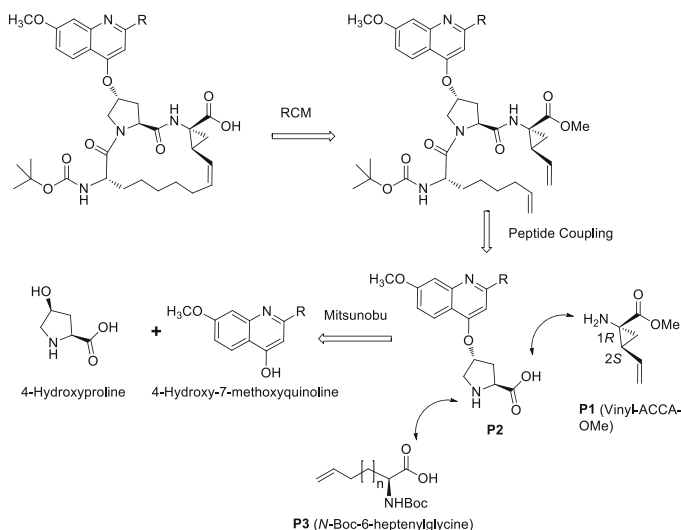
Fig. 3 Retrosynthesis of macrocyclic inhibitors of the HCV NS3/NS4A protease

3.1 Synthesis of the P1 Fragment (Vinyl ACCA)

Following the initial discovery of 1-aminocyclopropanecarboxylic acid (ACCA) as a desirable substitute of the cysteine residue found in the substrate-based ligands (Fig. 1; P1; C-terminus residue of **1**) [16, 17], a number of substituted ACCA analogs were explored, leading to the identification of (1*R*,2*S*)-1-amino-2-vinylcyclopropanecarboxylic acid (Fig. 3; vinyl-ACCA methyl ester; P1) as the optimum P1 moiety [17]. Vinyl ACCA confers exceptional potency to both the linear and the macrocyclic inhibitor of this class and has become a common structural feature of most (*if not all*) second-generation HCV NS3/NS4A inhibitors (e.g., Table 1; Fig 2).

At the start of our investigations, the synthesis of vinyl ACCA had been reported in the literature [23]. Literature precedence for the asymmetric and phase transfer-catalyzed α,α-dialkylation of glycine imines was also known [24–26]. However, the published protocols usually required the use of expensive chiral complexes in order to achieve good levels of enantioselectivity and were not considered suitable for large-scale production of this unusual amino acid. Consequently, the BI team begun to explore the development of a new methodology that was more suitable for large-scale production of vinyl ACCA, and after significant effort, the highly efficient preparation summarized in Scheme 1 was reported [27].

The sequential S_N2–S_N2' dialkylation of glycine with (*E*)-1,4-dibromobut-2-ene was pursued, and given the pK_a of ~19 for imine **16** (Hα), formation of the Cα anion was achieved under a variety of basic conditions [28]. The imine **16** was prepared in kilogram scales via condensation of benzaldehyde with the hydrochloride salt of ethyl glycinate (**15**) in the presence of a desiccant (Scheme 1). Following a simple
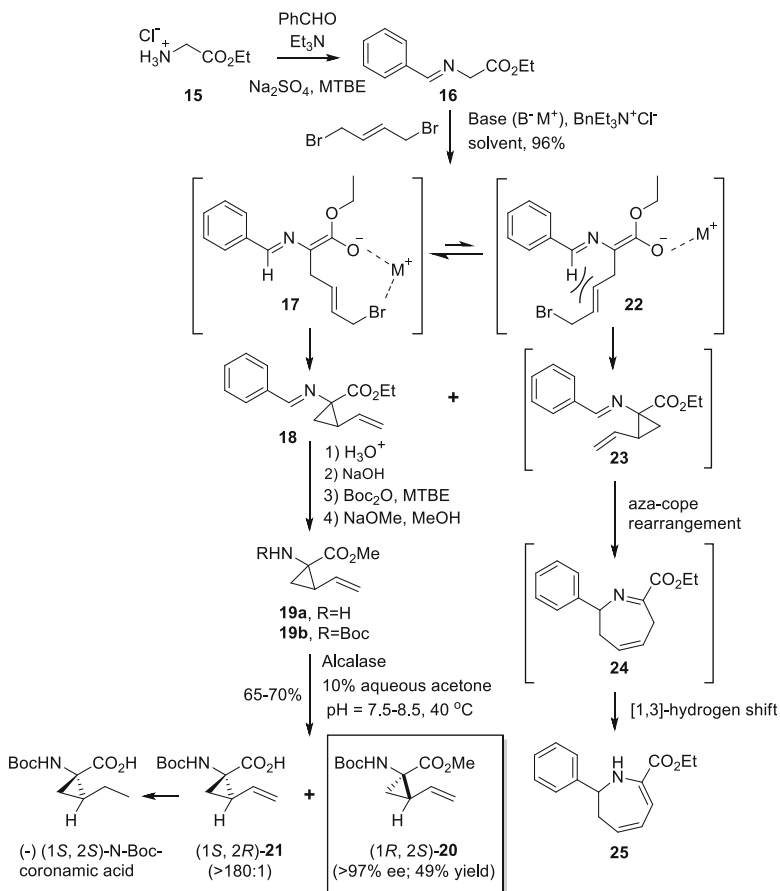
Scheme 1 Pilot plant synthesis of (1*R*, 2*S*)-1-amino-2-vinylcyclopropylcarboxylic acid methyl ester [**20**; (1*R*, 2*S*)-vinyl-ACCA-OMe]

aqueous workup, Schiff base **16** was isolated in 96% yield and was then treated directly with *trans*-1,4-dibromo-2-butene, in the presence of base and catalytic amounts of the phase transfer catalyst. The formation of the racemic mixtures of the two diastereomeric products **18** and **23** was anticipated. Surprisingly, after an acid/base workup of the crude reaction mixture, the racemic vinyl-ACCA ethyl ester **19a** (R=H) was isolated as a single diastereomer in 45% yield. The ^{1}H NMR data clearly indicated that the vinyl moiety was *cis* to the ester group (Scheme 1). Since this outcome was initially unexpected, the crude reaction mixture immediately after the cyclization step and before the acid/base workup (i.e., before cleaving the Schiff base) was analyzed by ^{1}H NMR. This study revealed the presence of two products, compound **18** and a second minor component, presumed to be intermediate **23** (Scheme 1). Further analysis of the organic layer collected post-cyclization and during the acidic aqueous workup led to the isolation of the

seven-membered ring side product **25**. Formation of compound **25** was rationalized to occur via the initial formation of the expected intermediate **23**, having the vinyl moiety *cis* to the imine. However, due to the geometry and functionality of this compound, a favorable and spontaneous aza-Cope rearrangement could occur to convert **23** to **24**, which upon [1,3]-hydride shift gave the final compound **25** (Scheme 1) [27].

In the initial reaction conditions for the sequential $S_N2–S_N2'$ dialkylation of **16**, excess powdered KOH and catalytic amounts of $BnEt_3N^+Cl^-$ (3%) as the phase transfer catalyst was used. The desired product **18** was formed, but with low diastereoselectivity (only a 3:1 ratio of the vinyl moiety *cis* to the ester versus *cis* to the imine was observed). Modifications of the imine **16**, which were previously reported to provide advantages in such reactions (e.g., replacing the benzaldehyde moiety with benzophenone) [29], were attempted without success and with a significant increase in the cost of raw materials. Similarly, replacement of the *trans*-1,4-dibromo-2-butene with other electrophiles did not provide any advantages. However, a systematic investigation of solvents, bases, and especially metal counterions that could stabilize the transition state enolate **17** proved to be extremely valuable. The reaction of **16** with *trans*-1,4-dibromo-2-butene in the presence of LiHMDS or *t*-BuOLi in a nonpolar solvent, such as toluene, led to the formation of the desired intermediate **18** in >40-fold higher yield as compared to **25** after 1 h. In contrast, more loosely coordinating metal ions (e.g., sodium or potassium), and/or the use of polar solvents (e.g., THF), led to the erosion of selectivity (**18**:**25** ratio of ~5±2:1). These observations suggested that the strongly coordinated *s-trans* transition state enolate **17** is favored in nonpolar solvents (and in the presence of the strongly coordinating lithium ion) leading to the desired product **18**, whereas the disfavored and sterically hindered enolate **22** (favored more in polar solvents) leads to the formation of the side product **25** (Scheme 1) [27].

Finally, the enzymatic resolution of the Boc-protected racemic product **19b**, using the inexpensive and commercially available *subtilisin Carlsberg* (Alcalase), provided the key building block (1*R*, 2*S*)-vinyl-ACCA methyl ester **20** in greater than 97% enantiomeric purity, along with the hydrolyzed enantiomer **21**. Assignment of the absolute stereochemistry of **21** was confirmed after hydrogenation to the ethyl analog, which proved to be identical to authentic (+)-(1*S*,2*S*)-*N*-Boc coronamic acid (Scheme 1) [27, 30].

3.2 Synthesis of the P2 Fragment

The synthesis of the P2 building block was initiated from 4-hydroxy-7-methoxy-quinolines, substituted at C-2 with various aromatic or heteroaromatic moieties, and 4-hydroxyproline (Fig. 3) [20]. It is noteworthy that although the C-2 substituent of the quinoline has minimal impact on the intrinsic potency of the macrocyclic inhibitors (IC_{50}), this moiety modulates significantly the cell-based antiviral
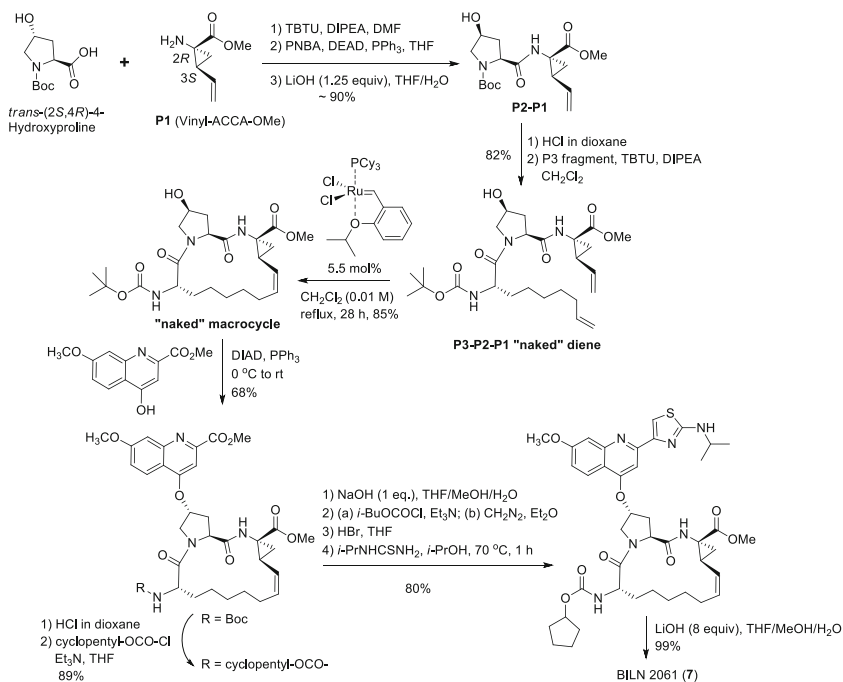
**Scheme 2** Initial assembly of BILN 2061 (**7**)

potency [31]. Therefore, a variety of quinolone moieties were coupled to the *cis*-4-hydroxyproline via the Mitsunobu reaction, proceeding with the expected inversion of stereochemistry at the C-4 of proline, to give the P2 fragment (Fig. 3) [16, 32, 33]. Alternatively, methyl 4-hydroxy-7-methoxyquinoline-2-carboxylate was coupled to the *cis*-4-hydroxyproline (via the Mitsunobu reaction), and the 2-carboxylate moiety was later modified to various heterocyclic analogs as part of our SAR studies, using various literature protocols.

However, the high cost of *cis*-4-hydroxyproline and its propensity to lactonize during the required peptide coupling reaction was a concern for the large-scale production of the P2 fragment. An alternative approach involved a double inversion of the stereochemistry at C-4 on the preformed macrocyclic scaffold (Scheme 2). Commercially available *trans*-(2*S*,4*R*)-Boc-hydroxyproline was first coupled with the methyl ester of the P1 fragment, (1*R*,2*S*)- vinyl-ACCA-OMe, using standard peptide coupling conditions. The resulting P1–P2 dipeptide was subsequently epimerized by first reacting the free C-4 hydroxyl of the proline with either *p*-nitrobenzoic acid or *p*-bromobenzenesulfonic acid via the Mitsunobu reaction, followed by regioselective hydrolysis of this moiety to afford the desired Boc-*cis*-(2*S*,4*S*)-4-hydroxyproline-(1*R*,2*S*)-vinyl-ACCA methyl ester [34]. The Boc group of the P1–P2 dipeptide was subsequently removed and coupled to the P3 amino acid to give the "naked" acyclic tripeptide diene (Scheme 2; P1–P2–P3 diene).

3.3 Synthesis of the P3 Fragment, (S)-2-Aminonon-8-enoic Acid

As part of our initial SAR studies, P3 fragments of various lengths and substitutions on the olefinic side chain were explored [20, 35]. A typical example of the synthetic methodology used for the P3 amino acid (2S)-N-Boc-6-heptenylglycine is shown in Scheme 3, Route A. The synthesis of the C-9 N-Boc-protected P3 (28; $n = 5$) was initiated from the 8-nonenoic acid (26), previously obtained after a Grignard reaction of the commercially available 8-bromo-1-octene with CO_2 [20, 35]. After coupling 26 with the chiral auxiliary (S)-4-benzyloxazolidin-2-one, the enolate was formed in the presence of KHMDS and reacted with 2,4,6-triisopropylbenzenesulfonyl azide (trisyl azide) to achieve the asymmetric azidation at the Cα position, as previously reported by Evans [36]. Reduction of the azide intermediate with $SnCl_2$ in methanol gave the corresponding free amine, which was protected as the t-butyl carbamates (Boc). Finally, the appropriately protected P3 fragment 28 was obtained in good yields after cleavage of the chiral auxiliary with LiOOH (Scheme 3, Route A). Although this synthetic approach (to the preparation of P3) was reasonable for our medicinal chemistry efforts, a methodology that was more atom economical and suitable for large-scale production of this fragment had to be developed in order to support the clinical development of BILN 2061 (7).

A sequence involving an enantioselective hydrogenation of the enamine 31 was pursued, as summarized in Scheme 3, Route B [33, 34]. Diethyl 2-acetamidomalonate was monohydrolyzed to intermediate 29, and the latter was coupled to 6-heptenal under Perkin conditions to give selectively the Z-ethyl 2-acetamido-2,8-nonadienoate 31 (50% yield) along with a small amount of the side product 30. At the same time, preparation of 31 via Horner–Wadsworth–Emmons olefination was also considered, but the so-called Perkin route was favored due to its simplicity. Intermediate 31 was subsequently enantioselectively hydrogenated using [(COD)Rh((S,S)-Et-DUPHOS)]OTf (catalyst load of ~0.1 mol %) to afford the ethyl (S)-2-acetamido-8-nonenoate in 99% enantiomeric excess and nearly quantitative yield [34]. The N-acetyl protecting group was replaced with
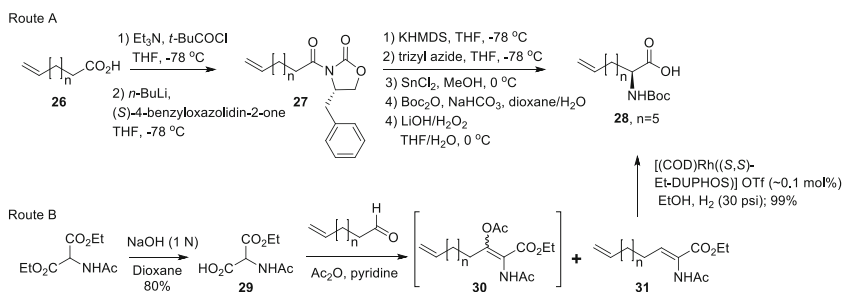

Scheme 3 Synthesis of P3 fragment

the *t*-butyl carbamate, and the ethyl ester was saponified using standard conditions, to give the P3 building block **28** (Scheme 2, Route B).

3.4 Challenges and Optimizations of the Ring-Closing Metathesis Reaction

As mentioned previously, the assembly of the 15-membered ring was initiated by coupling the three key amino acids (P1, P2, and P3), via standard peptide coupling conditions, to give an acyclic tripeptide diene (Scheme 2). However, in an effort to address a number of issues with the subsequent ring-closing metathesis (RCM) of this diene, various forms of the P1–P2–P3 tripeptide were explored, including the "naked" tripeptide diene shown in Scheme 2, as well as dienes **39** having various preassembled quinolones attached to the C-4 of proline, shown in Scheme 4. At the start of the program, the RCM reaction was attempted using the ruthenium-based catalysts known at that time, which were the Grubbs first-generation catalyst **32** and the Hoveyda catalyst **33** (Fig. 4). The backbone conformation of the acyclic diene precursor **39a** (Scheme 4), and in particular the *cis-/trans-*rotamer ratio of the proline amide bond (P2–P3 amide), was found to be crucial for the RCM reaction, as well as the diastereomeric purity of the macrocyclic product(s) formed [35]. Furthermore, the length of the olefinic side chain of P3 (used to modulate the ring size) had a profound effect on the diastereomeric purity of the macrocyclic product. For example, in the absence of the bulky *N*-Boc protecting group on the P3 nitrogen, or
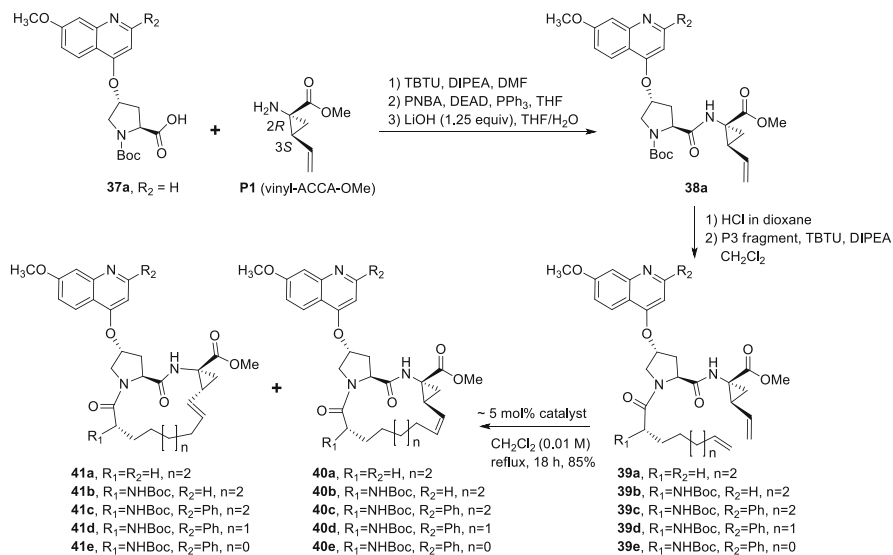
Scheme 4 Initial observation of the formation of macrocyclic products via the ring-closing metathesis reaction
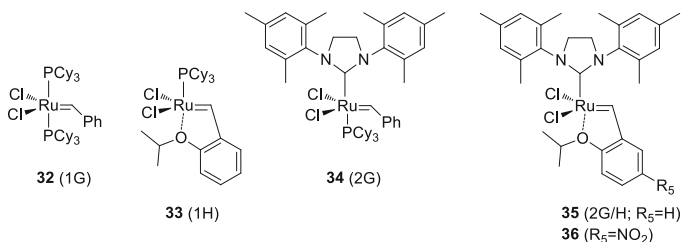
**Fig. 4** Ruthenium-based catalysts described in this study

in the absence of substitution at the Cα of the P3 fragment (e.g., Scheme 4; diene **39a**), the *cis-/trans*-rotamer ratio of the P2–P3 amide bond was approximately 1:1, and the outcome of the reaction was very poor, with only mixtures of product formed in <30% overall RCM conversion [35]. In contrast, the *cis/trans* ratio for diene **39b** (R_1=NHBoc) was approximately 1:9, thus pre-organizing the peptidic backbone to the β-strand conformation and mimicking the backbone of the desired macrocyclic product; evidently, this conformational pre-organization facilitated the RCM reaction. The overall conversion of diene **39b** to the 15-membered ring product **40b** was achieved in 40% yield using 5 mol% of catalyst **32** in refluxing CH_2Cl_2 (0.01 M solution) after approximately 2 h (~60% of total RCM conversion). Further improvement was observed using diene **39c**, which gave the desired diastereomer **40c** in 80% yield under the same RCM conditions (Scheme 4). These observations are analogous to those previously reported by Grubbs and coworkers on template-directed RCM reactions [37–39]. Remote control effects on the outcome of the RCM reaction were also reported in the synthesis of macrocyclic natural products, such as salicylihalamide [40, 41] and epothilones [42].

Interestingly, the RCM reaction of the acyclic dienes **39d** and **39e** proceeded almost exclusively via epimerization at the Cβ of the cyclopropyl ring and the formation of the 14-membered (**41d**) and 13-membered ring (**41e**) products, respectively (Scheme 4) [35]. Stereomutation at the Cβ of the vinyl cyclopropyl moiety of P1 (i.e., epimerization of the vinyl group from *cis* to *trans* with respect to the ester) was also detected in the RCM formation of the 15-membered ring (i.e., formation of **41b,c**), but only in very small amounts (<5% of the overall RCM product) [35].

Faced with the challenge of having to produce multi-kilogram quantities of BILN 2061 (**7**) and related analogs for clinical development, the RCM reaction had to be optimized extensively. The chiral integrity of the (1*R*,2*S*)-vinyl ACCA moiety (P1) was crucial in the conformation of the macrocyclic scaffold and, consequently, the affinity of these inhibitors for their intended biological target. Therefore, maintaining absolute stereochemical fidelity during the RCM cyclization of the diene was critical to the development of this class of compounds (Fig. 2; analogs **7–14**). Our initial evaluation of the factors that modulate the outcome of the RCM reaction (Scheme 4) suggested a Ru-mediated side reaction (from here on referred to as the *epi*-RCM pathway) involving the vinyl ACCA moiety [35, 43, 44].

This *epi*-RCM pathway was unprecedented in the literature, in spite of the fact that RCM reactions involving vinylcyclopropanes had been previously reported without any evidence of stereomutation; examples include the synthesis of radicicol-type macrolides [45, 46], coronanes [47], and oligo-*gem*-difluorocyclopropanes [48].

This led us to examine several Ru-based catalysts, including the Hoveyda catalyst **33** [49], and the imidazolium-based catalysts **34** and **35**, as well as the Grela catalyst **36** (Fig. 4) [50]. These catalysts typically provide higher turnover number (TON) [51–54], and their use appeared to resolve the issue of epimerization, at least on small-scale reactions. However, loss for chiral integrity, in addition to formation of cyclic dimers, resurfaced as a major issue when the RCM reaction was attempted on large scale, in spite of tight quality control of all starting materials, solvent, and reagents. For example, prewashing the reaction solvent with acid, in order to eliminate traces of amines and/or phosphines, became part of our large-scale protocol [55], but did not eliminate the epimerization issue. Since formation of minor side products that could not be easily removed from the active pharmaceutical ingredient (API) on a large scale was a major challenge for development, detailed mechanistic studies of the RCM reaction of various dienes with general structure **39** and **42** were investigated (Schemes 4 and 5). Other related issues were also essential to address, including (a) the cost of the required catalyst (initially 5–10 mol%), (b) the need to bring the levels of residual Ru metal in the final API to less than 10 ppm, and (c) the high volumes of solvent (i.e., low substrate concentration; <0.01 M) typically required for RCM reactions in order to avoid dimerization/polymerization. Failing to overcome these synthetic challenges could prohibit the production of BILN 2061 (**7**) in a pilot plant and consequently prevent further development of this important clinical candidate.
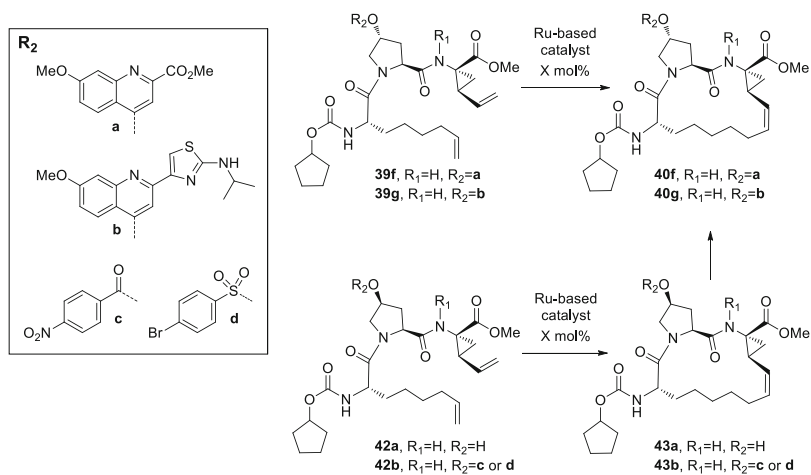
Scheme 5 Optimization of RCM reaction for the pilot plant synthesis of BILN 2061 (**7**)
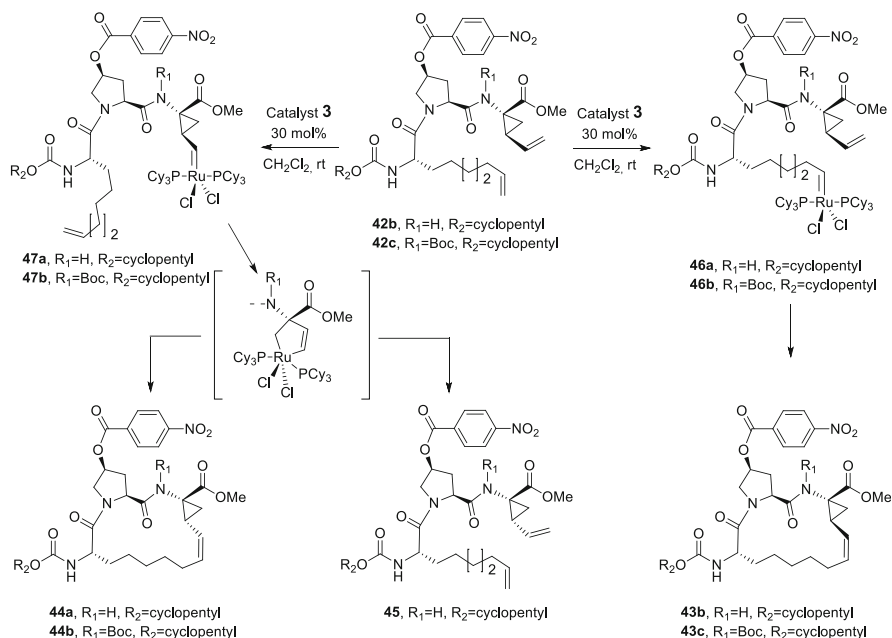
Scheme 6 Mechanistic pathway leading to the epimerization of vinyl ACCA and ways to block this pathway

Several complementary strategies for the assembly of substrate dienes **39** and **42** were carefully examined. This review cannot provide a complete and detailed account of all the studies undertaken during optimizations [43, 44, 55–57]. However, the critical effects of substitutions on the P1 nitrogen (R_1) and, to a lesser extent, the C-4 of the P2 proline moiety (R_2) in the outcome of the RCM reaction are summarized in Schemes 4, 5, and 6. Cyclization of dienes **39f** and **39g** (Scheme 5), already bearing the P2 quinoline construct and having the required stereochemistry at the C-4 of the proline, under RCM conditions gave very similar results to those observed previously with diene **39c** (Scheme 4). We also investigated the simpler dienes **42a,b**, having the C-4 hydroxyl of the P2 proline unprotected (**42a**) or temporarily protected as a benzoate or benzenesulfonate ester (**42b**), which can be activated post-cyclization for the introduction of the quinoline via S_N2 inversion (i.e., Mitsunobu reaction).

The relative efficiency of each substrate diene was evaluated in the RCM reaction under a variety of catalytic conditions. For the development of a scale-up/pilot plant-relevant protocol, all substrate dienes were used as the crude products obtained after the assembly sequence of the tripeptide dienes (i.e., post-peptide coupling of the P1, P2, and P3). Peptide synthesis of these dienes was typically achieved in high purity (>95% w/w), and further purification appeared to only affect the catalytic TON obtained in the RCM reaction and not the course or outcome of the reaction. There was only one important exception to these

observations in that the presence of even small amounts (as little as 1%) of phosphines or amines led to a significant increase in the amounts of epimerized product formed (Scheme 4; compound **41**), as discussed later.

Diene **42a** was thought to be a very desirable starting material, because it eliminated the need for protection/deprotection of the C-4 hydroxy of proline. However, the subtle conformational differences between dienes **42a** and **42b** proved to be sufficient to modulate the amounts of side products formed during the RCM reaction. For example, in contrast to the RCM reaction with diene **42a**, cyclization of diene **42b** proceeded uneventfully in excellent yield (90%) with Hoveyda catalyst **33** (3.5–5 mol%) at concentration of substrate of 10 mM in toluene at 60°C in 20–24 h without the formation of cyclic dimers (confirmed by LC–MS). Nonetheless, even these conditions were considered by the BI development team to be inadequate for the large-scale synthesis of BILN 2061 (**7**).

Cyclization of various forms of our tripeptide dienes under RCM conditions catalyzed by the more active Ru-based catalysts **34** and **35** was also evaluated. Although a catalyst load of only 0.5–1 mol% was sufficient to completely cyclize diene **42b** within 1–4 h, the desired product **43b** was contaminated with various cyclic dimers (accounting for ~8–10% of the overall yield), as well as the epimerized side product **44a** (Scheme 6). In the past, formation of non-metathesis side products has been observed in RCM reactions; these are often attributed to the decomposition of the ruthenium-based catalyst. Examples include ring contraction [58]; addition of chloroform to alkenes [59]; isomerization of allylamines, amides, and ethers [60–68]; and hydrogenation of the olefin [69, 70]. In some cases, understanding the mechanism of these side reactions has been proven to be valuable in developing new synthetic methodologies. Examples include the tandem RCM–alkene isomerization process for glycol synthesis developed by Snapper [65], the metathesis/hydrogenation process developed by Grubbs [69], and the RCM–double-bond migration reaction developed by Schmidt [71]. At that time, the epimerization of a vinylcyclopyl ring had not been previously observed in RCM reactions involving vinylcyclopropanes.

A Michael-type attack on the vinyl ACCA by the metal-dissociated PCy$_3$ ligand was ruled out, since epimerization was only observed at the Cβ carbon, whereas the stereochemistry of the Cα was unaffected under the RCM conditions. Furthermore, exposure of diene **39b** to PCy$_3$, under strict anaerobic and anhydrous conditions in refluxing CH$_2$Cl$_2$ over a period of 24 h, but in the absence of any Ru-based catalyst, failed to induce any epimerization of the vinyl ACCA (e.g., giving a product analogous to diene **45** in Scheme 6). It is noteworthy that all diastereomers of vinyl ACCA were previously isolated in high enantiomeric purity [27] and used independently in the synthesis of model tripeptide dienes. These compounds were independently used to study the epimerization phenomenon under RCM conditions, and the products formed were clearly distinguishable by their retention time on chiral HPLC, as well as their ^{1}H and ROESY NMR spectra. The results obtained from these model reactions confirmed that the mechanism of epimerization involved only the Cβ of the cyclopropyl ring and did not affect the Cα of the vinyl ACCA moiety.

A number of plausible mechanisms were considered that could involve a π-allyl-type shift of ruthenium hydride (formed as decomposition by-product of the catalyst) [72], an intermediate metal carbene or ruthenacyclopentene [35, 43] (formed via a metal-mediated expansion of the strained cyclopropyl ring) [73–77], or even an electron transfer oxidation mechanism [78]. Mindful of the ligands effects in modulating the reactivity and stereochemical outcome of the RCM/*epi*-RCM reactions, detailed kinetic studies and mechanistic investigations were undertaken. The tripeptide **42b** was subjected to RCM conditions with the first-generation Grubbs catalyst **32** (5 mol%) in toluene at 60°C, and the formation of **43b** and **44a** was observed in 1:1 ratio (Scheme 6). In addition, an isomer of the starting material, diene **45** was also observed [44]. However, when the Hoveyda catalyst **33** was used, under the same reaction conditions, the *epi*-RCM pathway was greatly suppressed giving less than 1% of the side products **44a** and **45**. Unfortunately, this initial observation turned out to be inconsistent from batch to batch, and occasionally product **44a** accounted for as much as 45% of the total RCM product. It was soon realized that competition between the RCM vs. the *epi*-RCM pathway was dependent on minor and variable impurities in the starting material.

A number of potential variables, including moisture, solvent, and substrate impurities, were analyzed by HPLC [44]. These studies revealed that small amounts of the free amine P1–P2 fragment **48** (as little as 1–2%) that escaped coupling with the P3 was in part responsible for catalyzing the *epi*-RCM pathway leading to the formation of **44a** and **45** (Scheme 6). To confirm this hypothesis, the RCM reaction was performed with highly pure diene **42b** in the presence of small amounts of **48** (Fig. 5) and independently with other basic amines (e.g., pyrrolidine and *N*-methylpyrrolidine) or an inorganic base (e.g., Cs_2CO_3). All amines tested promoted the epimerization reactions, whereas epimerization was not observed with the inorganic base. Similarly, various phosphines, such as PPh_3, PCy_3, and $P(n\text{-Bu})_3$, also promoted loss of chiral integrity, specifically at the Cβ of vinyl ACCA [44, 56, 57].

To gain further insight into the RCM vs. *epi*-RCM mechanisms, the reaction was subsequently carried out using a high load of catalyst **32** (30 mol%) in a deuterated solvent (CD_2Cl_2) at room temperature, and the progress was monitored by ${}^1H$ NMR. Two transient intermediate species, **46a** and **47a**, were detected, where the latter (**47a**) was the major species (~96%). After the initial formation of

Fig. 5 Structure of compound **48**

48
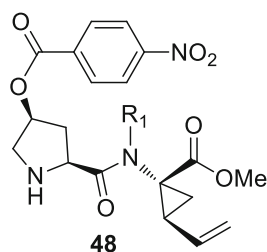
intermediate **47a**, its epimer at the Cβ of the cyclopropyl ring was also detected, and, simultaneously, the formation of products **44a** and **45** was observed. This surprising chemoselectivity for the more hindered olefin of diene **42b** could be driven by chelation of the Ru catalyst by the neighboring ester and amide bonds. It was presumed that substitution of the P1–P2 amide nitrogen with a bulky Boc group (Scheme 6; **42c**) might interrupt the coordination with the catalyst and redirect the Ru metal to the P3 side chain. This hypothesis was experimentally verified by ^{1}H NMR experiments, confirming that the cyclization of diene **42c** proceeded exclusively via intermediate **46b** leading to the desired product **43c**, without any evidence of intermediate **47b** in this reaction nor the formation of **44b**.

Further optimization of the RCM cyclization of diene **42c** and extensive catalyst screening (e.g., **34**, **35**, and **36**) led to the development of conditions that provide (a) higher yields, (b) lower reaction times, (c) much lower catalyst load, and (d) a dramatic improvement in the concentration required to achieve high yields of the desired product. For example, the formation of product **43b** decreased by 50% (from 85% to 35%) when the concentration of the precursor diene **42b** was increases by tenfold (from 0.01 to 0.10 M, respectively) if the RCM reaction was catalyzed by **36** (0.1 mol%). In contrast, cyclization of the *N*-Boc diene **42c** at 0.20 M concentration (at a 400 kg scale) using catalyst **36** (0.1 mol%) in toluene at 110 °C gave **43c** in 93% isolated yield (100% de; 100% conversion) after only 30 min. Furthermore, the superior robustness of catalyst **36** eliminated the need for oxygen sensors in the system, rendering the RCM reaction much easier to execute on a large scale. Additionally, although the epimerization reaction of the vinyl ACCA moiety can be avoided by acid-washing the solvents and using highly pure (>99%) dipeptide diene, by assuring that the reaction pathway proceed via intermediate **46b**, such precautions were no longer necessary for the RCM reaction. Finally, following the initial protocols for the preparation of BILN 2061 (**7**), the RCM reaction of 1 MT of the diene **42b** (e.g. Scheme 6) required as much as 150,000 L of solvent, whereas cyclization of the same amount of diene **42c** could be performed in only 7,500 L of solvent.

4 Conclusion

The stigma of poor drug-like properties associated with peptidomimetics, especially those that violate Lipinski's rules, is unlikely to be dispelled any time soon. Nonetheless, the 15-membered ring macrocyclic inhibitors of the HCV NS3/NS4A protease, which include the drugs simeprevir (**13**) and paritaprevir (**14**), are clearly an important class of antiviral agents for the treatment of HCV infection. From the perspective of modern medicinal chemistry, the *rational* design of these molecules was initially considered somewhat *irrational* by skeptics in the field of drug discovery (i.e., starting a discovery program from a hexapeptide lead with IC$_{50}$ of 800 μM). Perseverance by medicinal and process chemists, armed with insight gained from structural research on the factors influencing the pre-organization of

peptidic ligands to the bioactive conformation, led to the design of the β-strand macrocyclic core of the first clinically validated small molecule, BILN 2061 (**7**), that blocks HCV replication. However, the complex structure of BILN 2061, with three unnatural amino acids and five chiral centers, required considerable efforts in order to reach development status and enter clinical trials. This chapter provides a condensed summary of the most significant challenges and the key milestones in bringing this compound to clinical development. Collectively, overcoming the numerous obstacles in the design and synthesis of such a complex compound should be recognized as an important achievement not only in the development of BILN 2061 (**7**) but all the other analogs typified by the same 15-membered ring scaffold, having a vinyl ACCA moiety at P1. Evaluation/optimization of all the factors influencing the stereochemical integrity of the product during the key RCM macrocyclization step led to the first application of Ru-induced ring-closing metathesis in the pharmaceutical industry on multi-kilogram quantities.

References

1. Choo QL, Kuo G, Weiner AJ, Overby LR, Bradley DW, Houghton M (1989) Isolation of a cDNA clone derived from a blood-borne non-A, non-B viral hepatitis genome. Science 244:359–362
2. Tellinghuisen TL, Evans MJ, von Hahn T, You S, Rice CM (2007) Studying Hepatitis C virus: making the best of a bad virus. J Virol 81:8853–8867
3. Hadziyannis SJ, Papatheodoridis GV (2003) Effects of host and virus related factors on interferon-α+ ribavirin and pegylated-interferon+ribavirin treatment outcomes in chronic hepatitis C patients. Expert Opin Pharmacother 4:541–551
4. Chander G, Sulkowski MS, Jenckes MW, Torbenson MS, Herlong F, Bass EB, Gebo KA (2002) Treatment of chronic hepatitis C: a systematic review. Hepatology 36:S135–S144
5. Calcoen D, Elias L, Yu X (2015) What does it take to produce a breakthrough drug? Nat Rev Drug Discovery 14:161–162
6. Belema M, Lopez OD, Bender JA, Romine JL, St. Laurent DR, Langley DR, Lemm JA, O'Boyle II DR, Sun J-H, Wang C, Fridell RA, Meanwell NA (2014) Discovery and development of hepatitis C virus NS5A replication complex inhibitors. J Med Chem 57:1643–1672
7. Chen KX, Njoroge FG, Vibulbham B, Prongay A, Pichardo J, Madison V, Buevich A, Chan T-M (2005) Proline-based macrocyclic inhibitors of the hepatitis C virus: stereoselective synthesis and biological activity. Angew Chem Int Ed 44:7024–7028
8. Gale M Jr, Foy EM (2005) Evasion of intracellular host defence by hepatitis C virus. Nature 436:939–945
9. Chen KX, Njoroge FG (2009) A review of HCV protease inhibitors. Curr Opin Invest Drugs 10:821–837
10. Llinàs-Brunet M, Bailey M, Fazal G, Ghiro E, Gorys V, Goulet S, Halmos T, Maurice R, Poirier M, Poupart M-A, Rancourt J, Thibeault D, Wernic D, Lamarre D (2000) Highly potent and selective peptide-based inhibitors of the hepatitis C virus serine protease: towards smaller inhibitors. Bioorg Med Chem Lett 10:2267–2270
11. Ingallinella P, Altamura S, Bianchi E, Taliani M, Ingenito R, Cortese R, De Francesco R, Steinkühler C, Pessi A (1998) Potent peptide inhibitors of human hepatitis C virus NS3 protease are obtained by optimizing the cleavage products. Biochemistry 37:8906–8914
12. Schechter I, Berger A (1967) On the size of the active site in proteases. I. Papain. Biochem Biophys Res Commun 27:157–162

13. LaPlante SR, Cameron DR, Aubry N, Lefebvre S, Kukolj G, Maurice R, Thibeault D, Lamarre D, Llinàs-Brunet M (1999) Solution structure of substrate-based ligands when bound to hepatitis C virus NS3 protease domain. J Biol Chem 274:18618–18624

14. Cicero DO, Barbato G, Koch U, Ingallinella P, Bianchi E, Nardi MC, Steinkühler C, Cortese R, Matassa V, De Francesco R, Pessi A, Bazzo R (1999) Structural characterization of optimized product inhibitors with the N-terminal proteinase domain of the hepatitis C virus (HCV) NS3 protein by NMR and modelling studies. J Mol Biol 289:385–396

15. LaPlante SR, Aubry N, Bonneau PR, Kukolj G, Lamarre D, Lefebvre S, Li H, Llinàs-Brunet M, Plouffe C, Cameron DR (2000) NMR line-broadening and transferred NOESY as a medicinal chemistry tool for studying inhibitors of the hepatitis C virus NS3 protease domain. Bioorg Med Chem Lett 10:2271–2274

16. Poupart M-A, Cameron DR, Chabot C, Ghiro E, Goudreau N, Goulet S, Poirier M, Tsantrizos YS (2001) Solid-phase synthesis of peptidomimetic inhibitors for the hepatitis C virus NS3 protease. J Org Chem 66:4743–4751

17. Rancourt J, Cameron DR, Gorys V, Lamarre D, Poirier M, Thibeault D, Llinàs-Brunet M (2004) Peptide-based inhibitors of the hepatitis C virus NS3 protease : structure-activity relationship at the C-terminal position. J Med Chem 47:2511–2522

18. Lohmann V, Körner F, Koch J-O, Herian U, Theilmann L, Bartenschlager R (1999) Replication of subgenomic hepatitis C virus RNAs in hepatoma cell lines. Science 285:110–113

19. Tsantrizos YS, Bolger G, Bonneau P, Cameron DR, Goudreau N, Kukolj G, LaPlante SR, Llinàs-Brunet M, Nar H, Lamarre D (2003) Macrocyclic inhibitors of the NS3 protease as potential therapeutic agents of hepatitis C virus infections. Angew Chem Int Ed Engl 42:1356–1360

20. Tsantrizos YS, Cameron DR, Faucher A-M, Ghiro E, Goudreau N, Halmos T, Llinàs-Brunet M (2000) Macrocyclic peptides active against the hepatitis C virus. Boehringer Ingelheim (Canada) Ltd. WO Pat Appl 0,059,929A1

21. Lamarre D, Anderson PC, Bailey M, Beaulieu P, Bolger G, Bonneau P, Bös M, Cameron D, Cartier M, Cordingley MG, Faucher A-M, Goudreau N, Kawai SH, Kukolj G, Lagacé L, LaPlante SR, Narjes H, Poupart M-A, Rancourt J, Sentjens RE, St George R, Simoneau B, Steinmann G, Thibeault D, Tsantrizos YS, Weldon SM, Yong C-L, Llinàs-Brunet M (2003) An NS3 protease inhibitor with antiviral effects in humans infected with hepatitis C virus. Nature 426:186–189

22. Reiser M, Hinrichsen H, Benhamou Y, Reesink HW, Wedemeyer H, Avendano G, Riba N, Yong C-L, Nehmiz G, Steinmann GG (2005) Antiviral efficacy of NS3-serine protease inhibitor BILN-2061 in patients with chronic genotype 2 and 3 hepatitis C. Hepatology 41:832–835

23. Jiménez JM, Rifé J, Ortuño RM (1996) Enantioselective total syntheses of cyclopropane amino acids: natural products and protein methanologs. Tetrahedron Asymmetry 7:537–558

24. Ooi T, Takeuchi M, Kameda M, Maruoka K (2000) Practical catalytic enantioselective synthesis of α, α-dialkyl-α-amino acids by chiral phase-transfer catalysis. J Am Chem Soc 122:5228–5229

25. Belokon YN, Kochetkov KA, Churkina TD, Ikonnikov NS, Chesnokov AA, Larionov OV, Singh I, Parmar VS, Vyskocil S, Henri B, Kagan HB (2000) Asymmetric PTC C-alkylation catalyzed by chiral derivatives of tartaric acid and aminophenols. Synthesis of (R)- and (S)-α-methyl amino acids. J Org Chem 65:7041–7048

26. Belokon YN, Bhave D, D'Addario D, Groaz E, Maleev V, North M, Pertrosyan A (2003) Catalytic, asymmetric synthesis of α, α-disubstituted amino acids. Tetrahedron Lett 44:2045–2048

27. Beaulieu PL, Gillard J, Bailey MD, Boucher C, Duceppe J-S, Simoneau B, Wang X-J, Zhang L, Grozinger K, Houpis I, Farina V, Heimroth H, Krueger T, Schnaubelt J (2005) Synthesis of (1R,2S)-1-amino-2-vinylcyclopropanecarboxylic acid (Vinyl-ACCA) derivatives: key intermediates for the preparation of inhibitors of the hepatitis C virus NS3 protease. J Org Chem 70:5869–5879

28. O'Donnell MJ, Bennett WD, Bruder WA, Jacobsen WN, Knuth K, LeClef B, Polt RL, Bordwell FG, Mrozack SR, Cripe TA (1988) Acidities of glycine schiff bases and alkylation of their conjugate bases. J Am Chem Soc 110:8520–8525

29. O'Donnell MJ, Polt RL (1982) A mild and efficient route to schiff base derivatives of amino acids. J Org Chem 47:2663–2666

30. Charette AB, Côté B (1995) Stereoselective synthesis of all four isomers of coronamic acid: a general approach to 3-methanoamino acids. J Am Chem Soc 117:12721–12732

31. Llinàs-Brunet M, Bailey MD, Bolger G, Brochu C, Faucher A-M, Ferland JM, Garneau M, Ghiro E, Gorys V, Grand-Maître C, Halmos T, Lapeyre-Paquette N, Liard F, Poirier M, Rhéaume M, Tsantrizos YS, Lamarre D (2004) Structure-activity study on a novel series of macrocyclic inhibitors of the hepatitis C virus NS3 protease leading to the discovery of BILN 2061. J Med Chem 47:1606–1608

32. Tsantrizos YS (2004) The design of a potent inhibitor of the hepatitis C virus NS3 protease: BILN2061-from the NMR tube to the clinic. Biopolymers 76:309–323

33. Goudreau N, Brochu C, Cameron DR, Duceppe J-S, Faucher A-M, Ferland J-M, Grand-Maitre C, Poirier M, Simoneau B, Tsantrizos YS (2004) Potent inhibitors of the hepatitis C virus NS3 protease: design and synthesis of macrocyclic substrate-based β-strand mimics. J Org Chem 69:6185–6201

34. Faucher A-M, Bailey M, Beaulieu P, Brochu C, Duceppe J-S, Ferland J-M, Ghiro E, Gorys V, Halmos T, Kawai SH, Poirier M, Simoneau B, Tsantrizos YS, Llinàs-Brunet M (2004) Synthesis of BILN 2061, an HCV NS3 protease inhibitor with proven antiviral effect in humans. Org Lett 6:2901–2904

35. Poirier M, Aubry N, Boucher C, Ferland J-M, LaPlante S, Tsantrizos YS (2005) RCM of tripeptide dienes containing a chiral vinylcyclopropane moiety: impact of different Ru-based catalysts on the stereochemical integrity of macrocyclic products. J Org Chem 70:10765–10773

36. Evans DA, Evrard DA, Rychnovsky SD, Früh T, Whittingham WG, DeVries KM (1992) A general approach to the asymmetric synthesis of vancomycin-related arylglycines by enolate azidation. Tetrahedron Lett 33:1189–1192

37. Weck M, Mohr B, Sauvage J-P, Grubbs RH (1999) Synthesis of catenane structures via ring-closing metathesis. J Org Chem 64:5463–5471

38. Mohr B, Weck M, Sauvage J-P, Grubbs RH (1997) High-yield synthesis of [2] catenanes by intramolecular ring-closing metathesis. Angew Chem Int Ed Engl 36:1308–1310

39. Marsella MJ, Maynard HD, Grubbs RH (1997) Template-directed ring-closing metathesis: synthesis and polymerization of unsaturated crown ether analogs. Angew Chem Int Ed Engl 36:1101–1103

40. Fürstner A, Dierkes T, Thiel OR, Blanda G (2001) Total synthesis of (−)-salicylihalamide. Chem Eur J 7:5286–5298

41. Fürstner A, Thiel OR, Blanda G (2000) Asymmetric synthesis of the fully functional macrolide core of salicylihalamide: remote control of olefin geometry during RCM. Org Lett 2:3731–3734

42. Meng D, Su D-S, Balog A, Bertinato P, Sorensen EJ, Danishefsky SJ, Zheng Y-H, Chou T-C, He L, Horwitz SB (1997) Remote effects in macrolide formation through ring-forming olefin metathesis: an application to the synthesis of fully active epothilone congeners. J Am Chem Soc 119:2733–2734

43. Tsantrizos YS, Ferland J-M, McClory A, Poirier M, Farina V, Yee NK, Wang X, Haddad N, Wei X, Xu J, Zhang L (2006) Olefin ring-closing metathesis as a powerful tool in drug discovery and development-potent macrocyclic inhibitors of hepatitis C virus NS3 protease. J Organomet Chem 691:5163–5171

44. Zeng X, Wei X, Farina V, Napolitano E, Xu Y, Zhang L, Haddad N, Yee NK, Grinberg N, Shen S, Senanayake CH (2006) Epimerization reaction of a substituted vinylcyclopropane catalyzed by ruthenium carbenes: mechanistic analysis. J Org Chem 71:8864–8875

45. Yang Z-Q, Geng X, Solit D, Pratilas CA, Rosen N, Danishefsky SJ (2004) New efficient synthesis of resorcinylic macrolides via ynolides: establishment of cycloproparadicicol as synthetically feasible preclinical anticancer agent based on Hsp90 as the target. J Am Chem Soc 126:7881–7889

46. Yamamoto K, Biswas K, Gaul C, Danishefsky SJ (2003) Effects of temperature and concentration in some ring closing metathesis reactions. Tetrahedron Lett 44:3297–3299

47. Barrett AGM, Hamprecht D, James RA, Ohkubo M, Procopiou PA, Toledo MA, White AJP, Williams DJ (2001) Synthesis and characterization of coronanes: multicyclopropane-fused macrocyclic arrays. J Org Chem 66:2187–2196

48. Itoh T, Mitsukura K, Ishida N, Uneyama K (2000) Synthesis of bis- and oligo-*gem*-difluoro-cyclopropanes using the olefin metathesis reaction. Org Lett 2:1431–1434

49. Kingsbury JS, Harrity JPA, Bonitatebus PJ, Hoveyda AH (1999) A recyclable Ru-based metathesis catalyst. J Am Chem Soc 121:791–799

50. Michrowska A, Bujok R, Harutyunyan S, Sashuk V, Dolgonos G, Grela K (2004) Nitro-substituted Hoveyda-Grubbs ruthenium carbines: enhancement of catalyst activity through electronic activation. J Am Chem Soc 126:9318–9325

51. Scholl M, Trnka TM, Morgan JP, Grubbs RH (1999) Increased ring closing metathesis activity of ruthenium-based olefin metathesis catalysts coordinated with imidazolin-2-ylidene ligands. Tetrahedron Lett 40:2247–2250

52. Weskamp T, Kohl FJ, Hieringer W, Gleich D, Herrmann WA (1999) Highly active ruthenium catalysts for olefin metathesis: the synergy of *N*-heterocyclic carbenes and coordinatively labile ligands. Angew Chem Int Ed Engl 38:2416–2419

53. Huang J, Stevens ED, Nolan SP, Petersen JL (1999) Olefin metathesis-active ruthenium complexes bearing a nucleophilic carbene ligand. J Am Chem Soc 121:2674–2678

54. Garber SB, Kingsbury JS, Gray BL, Hoveyda AH (2000) Efficient and recyclable monomeric and dendritic Ru-based metathesis catalysts. J Am Chem Soc 122:8168–8179

55. Nicola T, Brenner M, Donsbach K, Kreye P (2005) First scale-up to production scale of a ring closing metathesis reaction forming a 15-member macrocycle as a precursor of an active pharmaceutical ingredient. Org Process Res Dev 9:513–515

56. Yee NK, Farina V, Houpis I, Haddad N, Frutos RP, Gallou F, Wang X-J, Wei X, Simpson RD, Feng X, Fuchs V, Xu Y, Tan J, Zhang L, Xu J, Smith-Keenan LS, Vitous J, Ridges MD, Spinelli EM, Johnson M, Donsbach K, Nicola T, Brenner M, Winter E, Kreye P, Samstag W (2006) Efficient large-scale synthesis of BILN 2061, a potent HCV protease inhibitor, by a convergent approach based on ring-closing metathesis. J Org Chem 71:7133–7145

57. Shu C, Zeng X, Hao M-H, Wei X, Yee NK, Busacca CA, Han Z, Farina V, Senanayake CH (2008) RCM macrocyclization made practical:An efficient synthesis of HCV protease inhibitor BILN 2061. Org Lett 10:1303–1306

58. Fürstner A, Thiel OR, Ackermann L, Schanz H-J, Nolan SP (2000) Ruthenium carbene complexes with N,N′-bis(mesityl)imidazol-2-ylidene ligands: RCM catalysts of extended scope. J Org Chem 65:2204–2207

59. Tallarico JA, Malnick LM, Snapper ML (1999) New reactivity from (PCy$_3$)$_2$Cl$_2$Ru=CHPh: a Mild catalyst for Kharasch additions. J Org Chem 64:344–345

60. Hu Y-J, Dominique R, Das SK, Roy R (2000) A facile new procedure for the deprotection of allyl ethers under mild conditions. Can J Chem 78:838–846

61. Cadot C, Dalko PI, Cossy J (2002) Olefin isomerization by a ruthenium carbenoid complex. Cleavage of allyl and homoallyl groups. Tetrahedron Lett 43:1839–1841

62. Hoye TR, Zhao H (1999) Some allylic substituent effects in ring-closing metathesis reactions: allylic alcohol activation. Org Lett 1:1123–1125

63. Alcaide B, Almendros P, Alonso JM, Aly MF (2001) A novel use of Grubbs' carbene. Application to the catalytic deprotection of tertiary allylamines. Org Lett 3:3781–3784

64. Wipf P, Rector SR, Takahashi H (2002) Application in total synthesis of (-)-tuberostemonine. J Am Chem Soc 124:14848–14849

65. Sutton AE, Seigal BA, Finnegan DF, Snapper ML (2002) New tandem catalysis: preparation of cyclic enol ethers through a ruthenium-catalyzed ring-closing metathesis–olefin isomerization sequence. J Am Chem Soc 124:13390–13391
66. Arisawa M, Terada Y, Nakagawa M, Nishida A (2002) Selective isomerization of a terminal olefin catalyzed by a ruthenium complex: the synthesis of indoles through ring-closing metathesis. Angew Chem Int Ed 41:4732–4734
67. Braddock DC, Matsuno A (2002) In situ tandem allylic acetate isomerisation-ring closing metathesis: 1,3-dimesityl-4,5-dihydroimidazol-2-ylidene ruthenium benzylidenes and palladium(0)–phosphine combinations. Tetrahedron Lett 43:3305–3308
68. Braddock DC, Wildsmith AJ (2001) On the use of tandem allylic acetate isomerisation and ring-closing metathesis with palladium(0) phosphine complexes and ruthenium benzylidenes as orthogonal catalysts. Tetrahedron Lett 42:3239–3242
69. Bielawski CW, Louie J, Grubbs RH (2000) Tandem catalysis: three mechanistically distinct reactions from a single ruthenium complex. J Am Chem Soc 122:12872–12873
70. Watson MD, Wagener KB (2000) Tandem homogeneous metathesis/heterogeneous hydrogenation: preparing model ethylene/CO_2 and ethylene/CO copolymers. Macromolecules 33:3196–3201
71. Schmidt B (2004) Catalysis at the interface of ruthenium carbene and ruthenium hydride chemistry: organometallic aspects and applications to organic synthesis. Eur J Org Chem 2004:1865–1880
72. Ulman M, Grubbs RH (1999) Ruthenium carbene-based olefin metathesis initiators: catalyst decomposition and longevity. J Org Chem 64:7202–7207
73. Jordan RW, Khoury PR, Goddard JD, Tam W (2004) Ruthenium-catalyzed [2+2] cycloadditions between 7-substituted norbornadienes and alkynes: an experimental and theoretical study. J Org Chem 69:8467–8474
74. Echavarren AM, Nevado C (2004) Non-stabilized transition metal carbenes as intermediates in intramolecular reactions of alkynes with alkenes. Chem Soc Rev 33:431–436
75. Trost BM, Pinkerton AB, Toste FD, Sperrle M (2001) Synthesis of 1,1-disubstituted alkenes via a Ru-catalyzed addition. J Am Chem Soc 123:12504–12509
76. Wender PA, Husfeld CO, Langkopf E, Love JA (1998) First studies of the transition metal-catalyzed [5+2] cycloadditions of alkenes and vinylcyclopropanes: scope and stereochemistry. J Am Chem Soc 120:1940–1941
77. Wender PA, Takahashi H, Witulski B (1995) Transition metal catalyzed [5+2] cycloadditions of vinylcyclopropanes and alkynes: a homolog of the Diels–Alder reaction for the synthesis of seven-membered rings. J Am Chem Soc 117:4720–4721
78. Dinnocenzo JP, Schmittel M (1987) Cyclopropane stereomutation catalyzed by one-electron oxidants. J Am Chem Soc 109:1561–1562